IEEE Access
Multidisciplinary | Rapid Review | Open Access Journal

Received 23 March 2023, accepted 13 April 2023, date of publication 17 April 2023, date of current version 27 April 2023.

Digital Object Identifier 10.1109/ACCESS.2023.3267802

RESEARCH ARTICLE

Online Tracking of Small-Signal Stability Rightmost Eigenvalue Based on Reference Point

XIN CUN, XUNJUN CHEN, (Member, IEEE), GUANGCHAO GENG, (Senior Member, IEEE), AND QUANYUAN JIANG, (Senior Member, IEEE)

College of Electrical Engineering, Zhejiang University, Hangzhou, Zhejiang 310027, China

Corresponding author: Guangchao Geng (ggc@zju.edu.cn)

This work was supported in part by the National Natural Science Foundation of China under Grant 51977188.

ABSTRACT Machine learning technologies have been applied to improve the real-time performance of small-signal stability assessment, while achieving a high accuracy requires numerous samples, and model performance may degrade if not updated over time. Furthermore, single models tend to learn general features without analyzing specific characteristics within the samples, which may lead to a high frequency of large errors, particularly at operating points where the eigenvalue trajectories have sudden changes. Facing such issues, this paper introduces the concept of reference points for accurate online tracking of the rightmost eigenvalue, as the reference points information reflects the characteristics among its surrounding operating points. The performance of this model is sensitive to reference points, so affinity propagation clustering is employed to determine the number of reference points and generate corresponding groups, accommodating diverse operating points characteristics. This paper generates data-driven networks for each group and combines them into a multi-network for precise rightmost eigenvalue prediction. Case studies show that the use of reference points improves accuracy by nearly 2% compared to methods without them, with even greater improvements in mixed load type scenarios. To mitigate computational stress, this paper proposes an adaptive partial update strategy based on the dynamic time warping algorithm, avoiding the need to update all networks within each sliding time window. Experimental results verify that the total running time is reduced by more than 10%. Online tracking demonstrates that reference points help decrease the frequency of large errors by 40%, especially at sudden change points of rightmost eigenvalue trajectories.

INDEX TERMS Adaptive partial update strategy, reference point, rightmost eigenvalue, online tracking, small-signal stability.

I. INTRODUCTION

Small-signal stability (SSS) is the prerequisite of security operation in the power system, especially as the interconnection of power grids and capacity growth continue to increase [1], [2], hence real-time SSS assessment has become an urgently requires. SSS is determined by the real part of rightmost eigenvalue (RE), which normally provides the essential information to improve the stability of power system. Therefore, the rapid and accurate tracking of RE in the ever-changing grid is an important task for power system security operation and control [3], [4], [5].

One classical approach to obtain RE is the eigenvalue analysis method, which calculates the whole eigenvalues or part of eigenvalues with poorly damping ratio by the linearized model of power system [6], [7], [8]. Although this method offers high accuracy, it is very time-consuming due to the typically large dimension of the linearized model. Moreover, it requires the detailed dynamic model, which may not be practical in fast time-varying grids. Another conventional approach is to identify RE from the time domain waveform of the power system, as provided by the phasor measurement unit (PMU) [9], [10], [11]. In comparison with the eigenvalue

The associate editor coordinating the review of this manuscript and approving it for publication was Ramazan Bayindir.

analysis method, this approach significantly improves the speed of RE identification. Whereas the measurement-based method normally extracts the necessary information after the disturbance has occurred, and the communication time delay may further affect the real-time performance.

Data-driven methods offer the most real-time solutions for SSS assessment, Table 1 compares the various methods discussed. Given the advantages and developments of machine learning technology, it has become increasingly popular to apply machine learning algorithms to address the SSS related problems. Data-driven classification models are convenient to predict stability labels [12], [13], while such approaches may not provide the information on oscillation modes at current OPs, such as frequency and damping. To obtain more oscillation mode information, some studies have used data-driven method to generate the linearized state matrix and calculate the eigenvalues [14], [15]. However, such method still suffers from the burden of computation. Therefore, some literatures address the critical eigenvalues at different OPs by arranging them to corresponding oscillation modes as output, while such method assumes the eigenvalue positions do not change abruptly, which is unrealistic in SSS problems due to the strong nonlinearity [16], [17], [18]. To tackle this issue, the researchers predicted the regions where the eigenvalues are located instead of the particular values, to improve the real-time performance of SSS assessment [19], while this method may result in overlapping eigenvalue regions.

TABLE 1. The comparison of SSS assessment methods.

Method	Core procedure	Stability assessment indicators
Eigenvalue analysis	Linearized model of power system[6][7][8]	RE/MDR
Measurement -based	Extract the information from time domain waveforms[9][10][11]	RE/MDR
Data-driven	Classification model[12][13]	Stability label
	Generate the linearized state matrix[14][15]	RE/MDR
	Output is the arranged oscillation mode[16][17][18]	MDR
	Output is the region of critical eigenvalues[19]	Region of RE
	Output is the RE or MD[20][21]	RE/MDR

As both the RE and the minimum damping ratio (MDR) directly determine the stability of the power system, several researches have focused on improving their accuracy, including the data-driven based model [20], [21]. Recent studies have utilized deep learning algorithms in SSS assessment [22], [23], while the accuracy performance of critical eigenvalues remains unsatisfactory. This paper concentrates on enhancing the accuracy of data-driven RE prediction, which is essential for the real-time SSS assessment, by introducing the concept of reference point (RP). Adopting the affinity propagation (AP) clustering to the proposed method, the given samples are divided into different groups and the central OP of each group is the RP. It is a flexible clustering method that can accommodate the different characteristics of OPs that can be reflected by each RP. Then, the particular networks in each group are established and combined to form the multi-network to reduce the error caused by the single network due to average learning. The generalized regression neural network (GRNN) is utilized as the network of the proposed model due to its nonlinear mapping capability and learning speed.

However, the behavior of the same power system may change significantly over time, this paper designs an online framework with the rolling update model to maintain the accuracy of the data-driven model for tracking RE. Most of existing online frameworks for SSS are measurement based methods [11], [24], however, such methods still suffer from high online computational burden as they normally require a high refresh rate of the sliding time window. Considering that the offline trained data-driven model naturally has extremely high real-time performance in online computation, a regular updating model is proposed in this paper. To alleviate the burden of refreshing all the multi-network in each sliding time window, this paper introduces an adaptive partial update strategy that calculates the similarity of each group of RPs in adjacent sliding time windows, by using dynamic time warping (DTW) algorithm. The network of one RP in the current sliding time window is able to directly adopt one of the networks in the last sliding time window, if its OPs have a high degree of similarity. Overall, the original contributions of this paper are as follow:

- The concept of RP is introduced to improve the accuracy of SSS RE estimation and to reduce the frequency of large errors, especially at OPs where the RE has sudden changes.
- An adaptive partial framework is designed to online tracking of RE with less computational burden and total running time.

The paper is organized as follows: the introduction of RP and the model of data-driven SSS RE based on RP are elaborated in Section II. In Section III, the online RE tracking framework with an adaptive partial update strategy is considered. The experimental results to verify the performance of the proposed paper are depicted in Section IV. Finally, the conclusion and future works are remarked in Section V.

II. SMALL-SIGNAL STABILITY RIGHTMOST EIGENVALUE TRACKING BASED ON REFERENCE POINTS

A. SMALL-SIGNAL STABILITY RIGHTMOST EIGENVALUE

The dynamic model of the power system can be represented by the differential algebraic equations (DAEs) as (1):

$$\begin{cases} \dot{\boldsymbol{x}} = \boldsymbol{f}(\boldsymbol{x}, \boldsymbol{y}) \\ 0 = \boldsymbol{g}(\boldsymbol{x}, \boldsymbol{y}) \end{cases} \tag{1}$$

where $\boldsymbol{x}$ and $\boldsymbol{y}$ represent the state variable vector and algebraic variable vector of power system, respectively. All equations in bold italics indicate matrices or vectors in the proposed paper.

The SSS in the power system is conventional assessed by Lyapunov linearization method, the stability of DAE is consistent with the linearization model in the neighborhood of (x_0, y_0) as (2):

$$\begin{bmatrix} \dot{\boldsymbol{x}} \\ 0 \end{bmatrix} = \begin{bmatrix} \nabla_x \boldsymbol{f} & \nabla_y \boldsymbol{f} \\ \nabla_x \boldsymbol{g} & \nabla_y \boldsymbol{g} \end{bmatrix} \begin{bmatrix} \Delta x \\ \Delta y \end{bmatrix}_{(x_0, y_0)} \tag{2}$$

Therefore, the stability of (2) is able to be represented as the state matrix $\boldsymbol{A} = \nabla_x \boldsymbol{f} - \nabla_y \boldsymbol{f} (\nabla_y \boldsymbol{g})^{-1} \nabla_x \boldsymbol{g}$. The eigenvalues of $\boldsymbol{A}$ are depicted as (3):

$$\begin{cases} \lambda_i = \sigma_i \pm j\omega_i \\ \xi_i = -\sigma_i / \sqrt{\sigma_i^2 + \omega_i^2} \end{cases} \tag{3}$$

where σ_i and ω_i represent the i-th real part and imaginary part of eigenvalues, respectively. Each pair of complex eigenvalues corresponds an oscillatory mode. ξ_i represents the i-th damping ratio of eigenvalues.

The eigenvalue with the maximum σ_i reflects the SSS of this OP, which is called the rightmost eigenvalue (RE) λ_r in the proposed paper:

$$\begin{cases} \lambda_r = \sigma_r \pm j\omega_r \\ \sigma_r = \max(\sigma_i) \end{cases} \tag{4}$$

The RE of power system is a crucial index for determining the stability, as instability occurs when the real part of RE exceeds 0. In addition, the RE and its eigenvector are able to provide the useful information to improve the stability in the control of SSS. Therefore, the accurate tracking RE has become an increasing demand for real-time SSS problems. Researchers have explored the use of machine learning technologies to establish the mapping relationship between the state or algebraic variables of power system and the eigenvalues. Although some machine learning approaches can handle linear or weakly nonlinear models, accurately estimating RE in strongly nonlinear power system remains a challenge when relying on those technologies alone.

B. REFERENCE POINTS

1) THE DESCRIPTION OF REFERENCE POINTS

To address such issues, the proposed paper introduces the concept of RPs to help track RE accurately. An OP is able to represented by a set of variables $\boldsymbol{X}$ as shown in (5):

$$\boldsymbol{X} = [x_1, x_2, \ldots, x_n] \tag{5}$$

where x_n is able to be represented the variables in the given power system, such as the power of generators, the parameters of excitation system, load level.

In order to demonstrate the concept of RP more clearly, $\boldsymbol{X}$ with high dimension is abstracted into a two-dimensional coordinate system in Fig.1, all the OPs locate in the range of variables.

In data-driven model, the connection of similar samples is clearly stronger than other samples, so the overall accuracy of multi-network containing different groups of similar OPs is better than the single rough network using all the samples. Inspired by this, our paper divides the OPs within the possible operating range into several groups, such as zone A in Fig. 1, based on their similarities. Moreover, information from one OP is able to contribute to the stability assessment of its surrounding OPs. Therefore, our paper selects the central OP in each group as the RP, as the yellow OP in the Fig. 1. The new OP is able to be judged by the RP whether it belongs to the corresponding group. Obviously, the number of RPs affects the accuracy of multi-network.

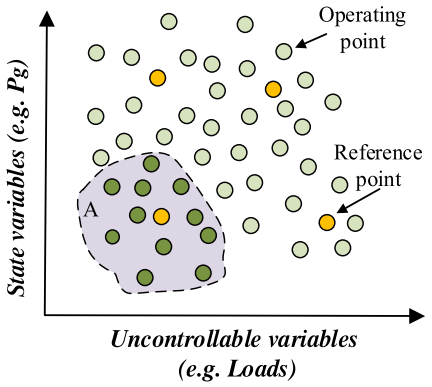

FIGURE 1. The diagram of reference points.

Whereas OPs are difficult and unnecessary to represent using the entire set of state variables due to the large dimensionality resulting from increased power system interconnection. The generator parameters are critical to the SSS problems, so the proposed paper selects the output of generators to represent the OPs. Furthermore, similar generator outputs may express different power system operation behavior at different time. Therefore, the generator outputs $\boldsymbol{P}_g$ with time labels $\boldsymbol{t}$ are represented to the OPs, (5) can be changed into (6).

$$\boldsymbol{X} = [\boldsymbol{P}_g, \boldsymbol{t}] \tag{6}$$

2) THE WAY TO DETERMINE THE REFERENCE POINTS

The determination of RPs is evidently crucial for the effectiveness of the proposed model. The number of RPs is equal to the number of multi-network. If the number of RPs is too small, the accuracy of the model may not be satisfactory. In fact, if only one RP is selected, the proposed model would become the data-driven model without RPs. However, selecting too many RPs is also inappropriate. With a fixed total sample size, a larger number of RPs will result in fewer OPs in each group, thus insufficient training samples may lead to greater error of network. Moreover, increasing the number of trained networks results in a proportional increase in network training parameters and computation costs, which reducing the real-time performance of RE prediction. Additionally, the number and location of RPs in different sliding time windows may vary due to the different characteristics of the data.

Therefore, the proposed online framework with streaming data requires an effective clustering method to pick up the RPs from its surrounding OPs. The classical clustering

methods are unsuitable as they normally require determine the number of clusters in advance. Since the number of RPs in the proposed updating model may vary due to different samples, it is inflexible and inaccurate to fix the number of clusters in advance. AP clustering, as one of the superior graph clustering methods, is selected as the proposed method to determine the RP, since the number of clusters is adaptive. AP clustering selects the center of clusters by exchanging messages between different points in the iterative process [25]. In addition, this approach is advantageous as the center of the cluster (RP) do not need to be newly generated OPs.

TABLE 2. Determination of reference points using AP clustering.

Algorithm 1: RPs determination

1: Compute similarity $s(i,k)$ by (7)
2: Initial $a(i,k)$ and $r(i,k)$ as 0 matrix.
3: $l = 1$
repeat
4: Update $r_{l+1}(i,k)$ by (8)
5: Update $a_{l+1}(i,k)$ by (9)
6: Damping $r_{l+1}(i,k)$ and $a_{l+1}(i,k)$ by (10)
7: $l = l + 1$
until $l > l_m$ or matrix $r_{l+1}(i,k)$ and $a_{l+1}(i,k)$ are stable

The process of RP determination using AP clustering is demonstrated in Table 2. The first step is to calculate the similarity between OPs. Each OP can generate a topology with pairwise connections, as shown in the upper-right corner of Fig. 2, n is the node number of the topology. Then based on the topology, the similarity matrix can be extracted to express the distance of each OP. The similarity matrix is demonstrated on the left of Fig. 2, the darker the color block, the closer the two OPs are.

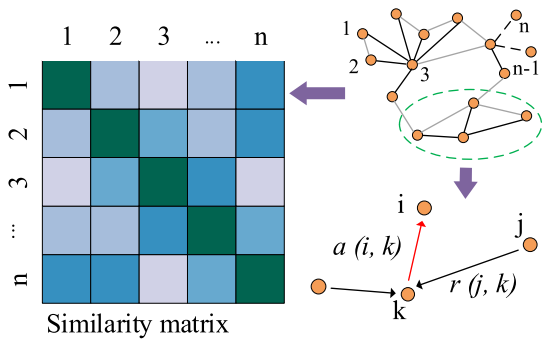

FIGURE 2. The diagram of AP clustering parameters.

The negative Euclidean distance is used to measure the similarity in AP clustering, while it is useless for the data with inconsistent scales between dimensions, just like the OP in (6). The numerical dimensions of generator outputs and time labels are obviously different. Therefore, standardized Euclidean distance is adopted to measure the similarity $s(i,k)$ of point i and k:

$$\boldsymbol{X}^* = (\boldsymbol{X} - \mu)/\delta$$
$$s(i,k) = -\sqrt{\sum_{n=1}^{2}(x_{in}^* - x_{kn}^*)^2/\delta_n} \tag{7}$$

where $\boldsymbol{X}^*$, μ and δ represent the standardized value, mean value and standard deviation of OPs, respectively.

The AP clustering first considers all the OPs as the candidate exemplar (cluster centers), then initializes the matrices of responsibilities $r(j,k)$ and availabilities $a(i,k)$ at step 2 in the Table 2. $r(j,k)$ represents the degree to which point k is suitable to be the cluster center of point j, $a(i,k)$ represents the suitability of point i to select point k as its cluster center. The final centers are determined according to the addition of these two parameters.

In the iterative process of AP clustering in Table 2, the $(l+1)$-th iteration of responsibilities $r_{l+1}(j,k)$ and availabilities $a_{l+1}(i,k)$ are given in (8) and (9):

$$r_{l+1}(j,k) = \begin{cases} s(j,k) - \max_{i \neq k}[a_l(j,i) + r_l(j,i)], j \neq k \\ s(j,k) - \max_{i \neq k}[s(j,i)], j = k \end{cases} \tag{8}$$

$$a_{l+1}(i,k) = \begin{cases} \min[0, r_{l+1}(k,k) \\ \quad + \sum_{j \neq i,k} \max[r_{l+1}(j,k), 0]], i \neq k \\ \sum_{j \neq k} \max[r_{l+1}(j,k), 0]], i = k \end{cases} \tag{9}$$

A damping factor $\eta \in (0, 1)$ is introduced to update the $r_{l+1}(j,k)$ and $a_{l+1}(i,k)$ as shown in (10):

$$\begin{cases} r_{l+1}(j,k) = \eta r_l(j,k) + (1-\eta) r_{l+1}(j,k) \\ a_{l+1}(i,k) = \eta a_l(i,k) + (1-\eta) a_{l+1}(i,k) \end{cases} \tag{10}$$

AP clustering is terminated if the maximum number of iterations is greater than a threshold l_m or the $r(j,k)$ and $a(i,k)$ are not changed during the iteration process. Although AP clustering has a higher computational complexity than classical clustering methods, such disadvantage is able to be ignored when dealing with a small sample set. In addition, AP clustering is not sensitive to the initial samples and produces smaller error in cluster result than other clustering method like K-means. The length of sliding time window is short in the proposed online framework and requires high accuracy in determining RPs, so the proposed paper adopts AP clustering is reasonable and effective.

C. THE PROPOSED MULTI-NETWORK

Within a sliding time window extracted from the data stream, it is necessary to generate small networks in each group after dividing the OPs into suitable groups and determining the corresponding RPs, as described in the previous section. Figure 3 illustrates this process. The input and output of the proposed networks are the power of all the generators and the RE, respectively.

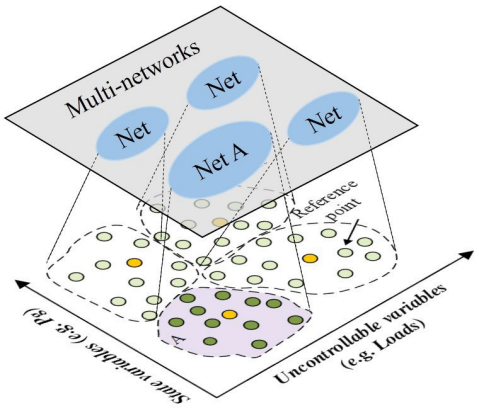

FIGURE 3. The proposed multi-network.

Unlike the conventional models where a single network is trained using all available samples, the proposed multi-network is composed of some small networks as demonstrated in Fig. 3. Several machine learning algorithms, such as ANN, support vector machine (SVM), convolutional neural network (CNN), and etc., can be considered as the potential network. Deep learning algorithms are known for their superior learning ability in handling nonlinear models and improving accuracy, but require a larger number of trained parameters and computation time to some extent.

To select the appropriate algorithm for the proposed method, we initially focus on shallow machine learning algorithms with fewer training parameters. Among them, GRNN seems to be a good choice to be the supporting network in the proposed method due to its strong nonlinear mapping ability and learning speed, especially in the case of a small sample set.

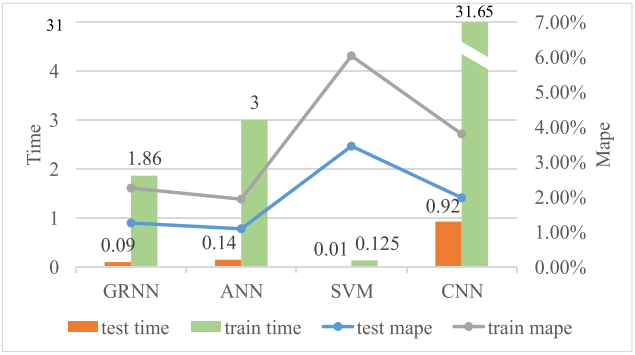

FIGURE 4. The comparison of different machine learning algorithms.

To verify this assumption, a case study is demonstrated in the Fig. 4, by using the generated samples (960 OPs) of the WSCC 9-bus test system, 70% for training and the rest for testing (same samples as the case study in the Section IV-A). In fact, the accuracy of such algorithms is similar. It can be clearly shown that regardless of the training time and testing time, the performance of CNN is much worse than other three algorithms, owing to its large number of parameters. As for the shallow machine learning algorithms, although the learning speed of SVM is faster than GRNN and ANN, the error of the former is larger than the latter, the reason of it may be the SVM is better suited for classification problem rather than regression problem. The learning speed of GRNN is faster than that of ANN, although the accuracy of them is similar. Overall, it is reasonable to choose GRNN as the supporting machine learning algorithm for the proposed paper.

GRNN is composed of four layers: input layer, pattern layer, summation layer and output layer. One of the advantages of GRNN is that it has fewer tunable parameters, usually limited to the value of spread. However, if the value of spread is set to be too large or too small, it may lead to poor accuracy or overfitting of the network training. The algorithm selection and tuning are not the main focus of this paper, besides, the accuracy of GRNN remains stable within a certain range of the spread value.

Therefore, considering the different characteristics of samples, the proposed paper provides a simple method to find a suitable value of spread. Firstly, the initial value of spread is set as 1 and then reduced by a multiple of 10 to observe the performance of network. If the training set accuracy is much higher than the test set, overfitting may have occurred; secondly, the value of spread is fine-tuned to this order of magnitude, for instance, the order of magnitude of the negative power of 10, then the value of spread is gradually reduced by 0.1 until the test set accuracy starts to show an upward trend; finally, after comparing the performance of the indicators, such as accuracy and testing time, which the user is more concerned about, a spread value within the better range can be selected.

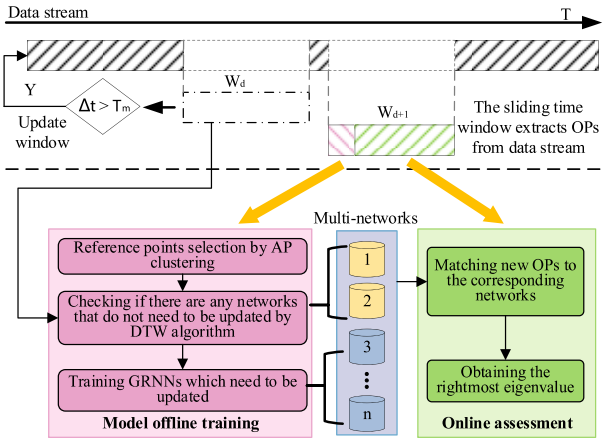

FIGURE 5. Online tracking of small-signal stability rightmost eigenvalue flowchart.

III. ONLINE TRACKING FRAMEWORK

This paper proposes a framework for the online tracking of SSS RE, the flowchart is shown in Fig. 5. The sliding time window extracts OPs from the data stream and updates from $\mathbf{W}_d$ to $\mathbf{W}_{d+1}$ in a regular time length as (11):

$$\Delta t \geq T_m \tag{11}$$

where Δt represents the time gap of last sliding time window and the current sliding time window. T_m represents the time threshold of updating the sliding time window.

A. ONLINE DATA MATCHING REFERENCE POINTS

As shown in Fig. 5, the data within one sliding time window is divided into two parts, one for offline model training model and the other for online RE tracking. In the offline stage, RPs are firstly selected using the AP clustering method which is depicted in the Section II-B. Then, the RPs from the last sliding time window are compared to the current RPs to determine whether any networks need not be trained. The detailed description of this partial update method is given in the following Section III-B. The remaining RPs and their surrounding OPs are used to train new GRNNs. These newly trained networks (network *3* to *n* in the Fig. 5), along with suitable networks (network *1* and *2* in the Fig. 5) transferred from the last sliding time window $\mathbf{W}_{\mathrm{d}}$, are combined to form the new multi-network for the current sliding time window for online assessment.

The other OPs of the current sliding time window $\mathbf{W}_{\mathrm{d+1}}$ are used for the online prediction of SSS RE, as can be visualized in Fig. 5. Firstly, it is necessary to determine to which group the new OPs belong. By calculating the standard Euclidean distance between new OPs and each RP, the RP with the minimum distance is identified as the group to which the OPs belong as (12):

$$G_j = g_j(\min([D_1, D_1, \ldots, D_n])) \tag{12}$$

where G_{j} represents the label of the group to which the j-th OP, the function $g(\cdot)$ represents get the index number, D_{i} represents the standard Euclidean distance between the new OP and i-th RP.

Finally, the generator power of the new OP as the input of the corresponding network, thus, the RE of the OP can be quickly obtained.

B. ADAPTIVE PARTIAL UPDATE STRATEGY

The proposed model utilizes a regular update strategy which is inflexible and may consume much unnecessary computational time due to frequent updates. To address such issues, an adaptive partial update strategy is introduced in the proposed model is given in Fig. 6. If the input of one network is similar to another one, then the two networks which trained by each input and output are also similar, which means that such samples belong to the same group. Therefore, in order to better utilize the historical information of the networks, the proposed adaptive partial update strategy reduces the number of networks needed to be updated, thus saving computational resources.

In the Fig. 6, both of the OPs extracted from current and last sliding time window are divided into several groups by AP clustering, a group consists of one RP and its surrounding OPs. To determine if there are any trained networks in the last window that can be directly transferred into the current window, the similarity of the current RPs to the last RPs

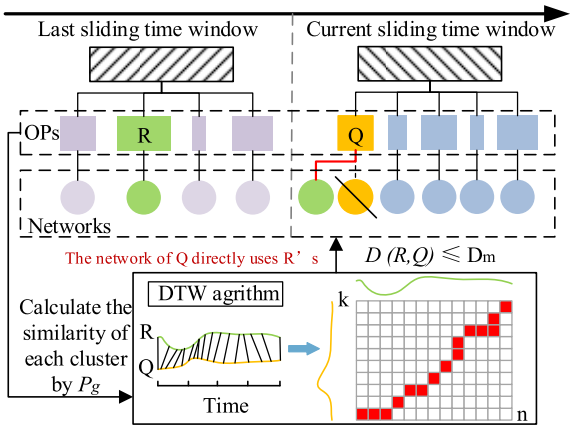

FIGURE 6. The diagram of adaptive partial update strategy.

is compared. However, conventional similarity comparative method requires same size, which is contrary to the proposed approach since the size of each group is normally different, such as the group $\boldsymbol{R}$ and $\boldsymbol{Q}$ in the Fig. 6. To remove the limitation, this paper chooses dynamic time warping (DTW) algorithm, as it is adept in measuring the similarity of two time series with different length. An example is given in the Fig. 6 to demonstrate the application of DTW algorithm, $\boldsymbol{R}$ and $\boldsymbol{Q}$ can be represented as (13)

$$\begin{aligned} \boldsymbol{R} &= [P_{g1}, P_{g2}, \cdots, P_{gn}] \\ \boldsymbol{Q} &= [P_{g1}, P_{g2}, \cdots, P_{gk}] \end{aligned} \tag{13}$$

where n and k represent the length of $\boldsymbol{R}$ and $\boldsymbol{Q}$, respectively. P_{g} represents the vector of generator outputs.

A distance matrix of size $n \times k$ is used to compare the similarity of $\boldsymbol{R}$ and $\boldsymbol{Q}$ in Fig. 6. The object of DTW algorithm is to find an optimal warping path (red squares) that goes across this matrix as (14):

$$\begin{aligned} \boldsymbol{D}(\boldsymbol{R}, \boldsymbol{Q}) = \min & \sqrt{\sum_{j=1}^{J} d_j} \\ \text{s.t.} & \begin{cases} d_1 = (1, 1), d_J = (n, k) \\ d_j - d_{j-1} = (\Delta n, \Delta k), 0 \le \Delta n \le 1, \\ \quad 0 \le \Delta k \le 1 \end{cases} \end{aligned} \tag{14}$$

where $d_j = (n, k)_{\mathrm{j}}$ represents the j-th element of the optimal warping path, the horizontal and vertical coordinates of d_j represent the corresponding point of $\boldsymbol{R}$ and $\boldsymbol{Q}$, respectively. Generally speaking, the constraint conditions mean that the warping path should subject to the boundary condition, continuity, and monotonicity.

Dynamic programming algorithm is adopted to solve (14) as (15):

$$\begin{aligned} \gamma(n, k) = & d(n, k) \\ & + \min\{\gamma(n-1, k-1), \gamma(n, k-1), \gamma(n-1, k)\} \end{aligned} \tag{15}$$

where $\gamma(n,\ k)$ represents the cumulative sum of optimal warping path at element $(n,\ k)$ in the distance matrix.

Hence, the similarity of $\boldsymbol{R}$ and $\boldsymbol{Q}$ can be calculated according to (13)-(15), if the similarity $\boldsymbol{D(R,\ Q)}$ is smaller than a threshold D_m, the sample of Q does not require new network training but can adopt the network of $\boldsymbol{R}$ directly as demonstrated in the Fig. 6. The networks of the other RPs are able to be determined whether use previous networks in this way, or if the new networks should be trained as described in Section II-C. The adaptive partial update strategy is able to reduce the unnecessary updates, which can save the computational storage and time in the proposed online framework.

IV. CASE STUDIES

Two typical systems with different scales are investigated in this paper: WSCC 9-bus test system with 9 buses, 3 generators, 9 transmission lines, all generators use 4th-order model with 4th-order excitation system. IEEE 118-bus system with 118 buses, 54 generators, 186 transmission lines, all generators use 6th-order model with 4th-order excitation system. The polynomial loads are used in both test systems. Power System Analysis Toolbox (PSAT) [26] is used for data generation. All the tests are performed on a computer with Intel Core i3-8100 3.6GHz CPU, 16GB RAM.

The baseline steady-state power flow data of the test systems are taken from MATPOWER [27]. Based on these baseline data, one-year typical daily load curves (data step size is 15 minutes) are used to generate samples of case studies. The load types of the proposed paper include the constant power load and mixed load (mixture of constant power, constant current, and constant admittance load) are shown in (16) and (17), respectively:

$$\begin{aligned} P' &= C_P \\ Q' &= C_Q \end{aligned} \tag{16}$$

$$\begin{aligned} P'' &= A_p(U_n/U_N)^2 + B_p(U_n/U_N) + C_P \\ Q'' &= A_Q(U_n/U_N)^2 + B_Q(U_n/U_N) + C_Q \end{aligned} \tag{17}$$

where P_{n}, Q_{n}, and U_{n} represent the constant loads and voltage of n-th load bus, respectively. U_N represents the nominal voltage. A_{p}, B_{p}, and C_{p} represent the constant admittance load, constant current load, and constant active power as the percentage of the active power load, respectively; A_{Q}, B_{Q}, and C_{Q} have the similar meaning in the reactive power load.

In the proposed paper, each of the aforementioned three loads accounts for one-third of the mixed load. The proposed model and case studies are implemented using MATLAB.

A. EFFECTIVENESS OF REFERENCE POINTS

The proposed paper introduces the RPs in multi-network to enhance the RE tracking accuracy. To validate the effectiveness of RPs, 10-day generated samples (960 OPs) from the 9-bus test system were utilized, where 7-day data of samples were used for training and others for testing. Load types include constant power loads, and partial constant power loads replaced by mixed loads. In the constant power load scenario, 8 RPs are selected in this case study by the method based on AP clustering as demonstrated in Fig. 7, where the surrounding OPs are linked to the corresponding RPs (triangle mark) within their groups.

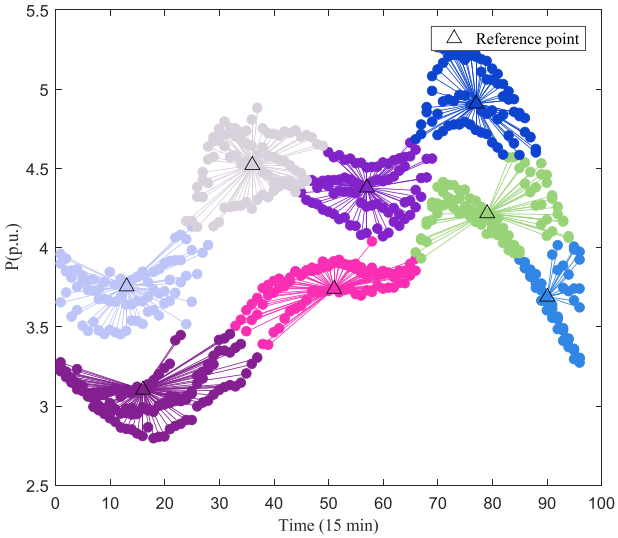

FIGURE 7. The reference points selected by the proposed method in 9-bus test system.

After selecting the RPs, the network of each group is trained by the corresponding RPs and the surrounding OPs. Table 3 lists the performance of different methods to validate the effectiveness of the RP. The REs calculated by the eigenvalue analysis method are considered as the accurate REs [26]. A two-layer data-driven method, the combination of hierarchical clustering (HC) and extreme gradient boosting (XGBoost), is introduced by [23] to obtain the REs and is also presented in this case study. In addition, Table 3 gives the result of the proposed method and the method without RPs, where the latter method trains one GRNN by using all the training samples. The proposed paper introduces two indexes to evaluate the performance of accuracy as (18): the mean absolute percentage error (Mape) depicts the numerical error and tracking performance of REs; error of stability (ES) measures the error of wrong stability assessment, which is the intolerable error in SSS problems.

$$\begin{aligned} Mape &= mean|(\lambda_{ra} - \lambda_{rp})/\lambda_{ra}| \times 100\% \\ ES &= N_f/N \times 100\% \end{aligned} \tag{18}$$

where λ_{ra} and λ_{rp} represent the actual and predicted RE, respectively. mean$(\cdot)$ is a function that averages the values inside the parentheses. N_f represents the number of OPs which the stability is false assessed, N represents the total number of OPs.

The experimental results presented in Table 3 demonstrate that all the data-driven methods for obtaining REs require significantly less testing time compared to the eigenvalue analysis method, with a minor reduction in accuracy, which

can be meet the real-time requirements of online RE tracking. Additionally, the ES values for all approaches are 0, which guarantees that the stability of the SSS will not be wrong. Although the accuracy of HC + XGBoost method is only slightly lower than the proposed model, its running time is nearly 4 times that of the latter, the reason may be that the parameters of ensemble learning is more than GRNN. The method without RPs takes less time than the proposed method, its accuracy is 1.85% lower in the constant power load scenario. Moreover, the accuracy performance of mixed load is worse than constant power load, obviously, when the load type is more complex, the ability of the data-driven model to establish the mapping of input and output diminishes. These results validate that the RPs do help to improve the performance of fast RE tracking.

TABLE 3. The effectiveness of reference points in 9-bus test system.

Load type	Method	Indices		
		Mape(%)	ES(%)	Time(s)
Constant power load	Eigenvalue analysis method [26]	0	0	136.11
	HC + XGBoost [23]	1.28	0	0.44
	Data-driven method without RPs	3.10	0	0.06
	Propose method	1.25	0	0.14
Mixed load	Eigenvalue analysis method [26]	0	0	148.58
	HC + XGBoost [23]	1.95	0	0.43
	Data-driven method without RPs	4.27	0	0.05
	Propose method	1.52	0	0.13

B. COMPARISON OF DIFFERENT NUMBER OF REFERENCE POINTS

As previously mentioned, the number of RPs in the proposed method has significant impact on its performance. However, determining the number of RPs in advance is inflexible and imprecise, especially in the online data stream. To demonstrate reasonableness of using AP clustering in this paper, a statistical analysis to the different number of RPs is displayed in this case study. The same samples from the previous case study are utilized, and a benchmark method uses the classical clustering method, k-means clustering, to fix the number of RPs in advance. The results of this case are presented in Fig. 8.

It can be seen from Fig. 8 that the more RPs, the longer the test time (the bar chart) and the smaller error (the line chart) of the model. Taking into account the aspects of test time and accuracy, the models with 7 and 8 RPs have better performance when using conventional clustering. To make a clearer comparison, the result from the previous case study using AP clustering is added in the Fig. 8 (two triangular markers in the circle). The proposed paper regards 8 is the optimal number of RPs, which aligns with the conclusion of the k-means clustering. The conventional cluster approaches typically faster than graph cluster approaches, so the test time of the proposed method is slightly longer than that of k-means clustering. However, the error of the former is smaller than the latter. In practical applications, the minor difference in time performance can be considered negligible, and the proposed reference point selection method offers greater flexibility in online RE tracking.

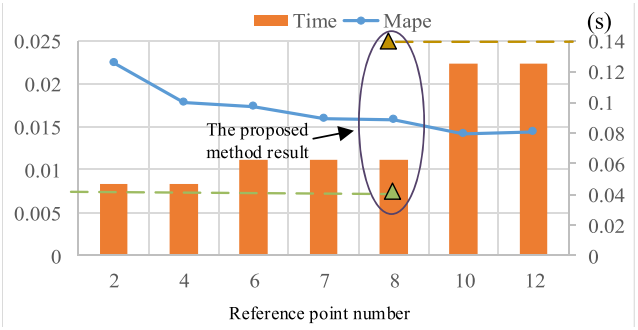

FIGURE 8. The benchmark performance of different number of reference points by using classical cluster method.

C. PERFORMANCE OF ONLINE TRACKING

The proposed method for online tracking of SSS RE is validated on a larger scale test system, the 118-bus system, using one-year generated samples where the load type scenario is mixed loads. The length of the sliding time window for the regular updating is 10 days, of which 8 days of data are used for offline training, the rest for online assessment. The RE tracking performance is demonstrated in Fig. 9 for a given day in the test dataset. The proposed method shows a RE trajectory that is very close to the actual value, outperforming the method without RPs, especially at the catastrophe point indicated by the ellipse in Fig. 9. The method without RPs assumes that REs change slowly between adjacent OPs, thus fails to capture the sudden changes in the RE trajectory. In fact, the REs sometimes have irregular movement due to the strong nonlinearity, so the introduction of RPs is effective in improving the performance of REs tracking.

The change of the error over one year is illustrated in the Fig. 10. To make it clearer, the average daily error is presented, with the proposed method consistently outperforming the data-driven method without RPs. The frequency of error exceeding 0.05 is also displayed, indicating that the proposed method has almost twice as many days with an error of less than 0.05 as the method without RPs. The above results demonstrate that the method proposed in this paper can better control the single-day error to a low level. Overall, RPs do help to reduce the error of online tracking for RE.

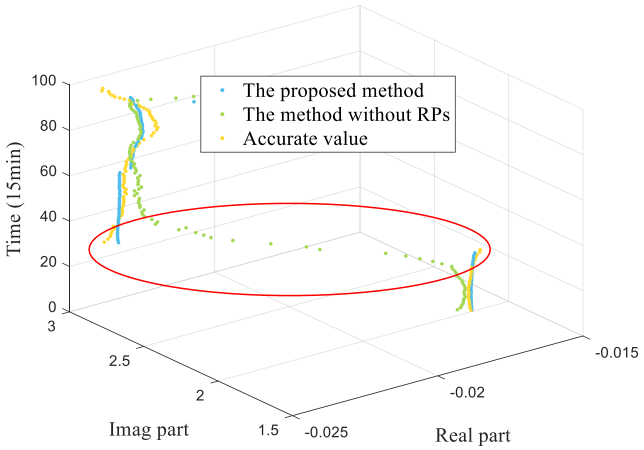

FIGURE 9. Rightmost eigenvalue online tracking performance in a given day.

TABLE 4. The effectiveness of adaptive partial update strategy in 118-bus system.

	Update all networks	Partial update networks	Performance improvement
Mape	4.16%	4.22%	-1.42%
ES	0%	0%	0%
Total running time (s)	32.75	29.40	+10.23%
Network training time(s)	11.81	6.81	+42.34%
Online test time (s)	2.52	2.33	+7.54%

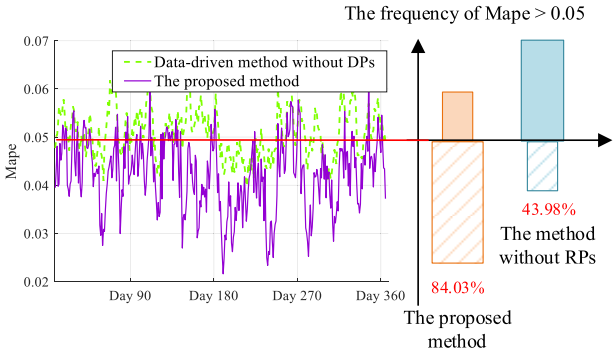

FIGURE 10. Error comparison between data-driven method with and without reference points.

D. PERFORMANCE OF ADAPTIVE PARTIAL UPDATE STRATEGY

To illustrate the effectiveness of the proposed adaptive partial update strategy, Table 4 brings the comparison between the model of updating all the networks and partial update networks in each updating period, by adopting the same samples in the last case study of 118-bus test system.

There are two error indexes and three indexes about time are listed in Table 4. Compared to the model that updates all networks, the total time performance of the partial updating networks is greatly reduced, despite slightly decreased accuracy. Notably, the network training time in all the updating periods of partial model is 42.34% less than that of the model that updates all networks. Although the partial model takes a little time to calculate the similarity of adjacent RPs, the total running time of former is also 10.23% less than latter. Hence, the adaptive partial update model based on DTW algorithm is effective in avoiding the unnecessary network updating during the regular updates and saving much computation time for the online tracking framework in the proposed paper.

V. CONCLUSION

This paper brings an accurate online tracking framework for SSS RE based on data-driven. The main finding of this study is that the overall performance of multiple networks representing different characteristics of given samples is better than a single network using all the data, especially at OPs where the RE has sudden changes. This paper identifies the central OP of such network as RP, which is crucial to the performance of the proposed method. To determine the RPs and its surrounding OPs, the proposed method adopts a flexible approach, AP clustering. The multi-network of the proposed paper consists of networks trained by different groups, then the REs of online OPs are obtained by the corresponding networks. Although the online framework of this paper is regular updating, a partial update strategy is proposed to relieve the stress of refreshing all the networks in each sliding time window. The DTW algorithm is used to check whether any current RPs can directly use the networks in the previous time sliding window. The effectiveness of the proposed model is illustrated by using 9-bus test system and 118-bus system. The small-scale system verifies the determination method of RPs is reasonable in this paper, in addition, shows that using RPs improves the accuracy by nearly 2% and 2.75% compared to methods without them in constant power load type and mixed load type scenarios, respectively. The online case studies are demonstrated in the larger test system, validating that this work does improve the accuracy of RE tracking with total running time saving of 10%. Furthermore, the proposed model reduces the frequency of large errors occurring in a single day by 40% and captures sudden changes in RE. The future works of authors will focus on the impact of renewable energy uncertainty on SSS assessment, building upon the foundations established in this paper.

REFERENCES

[1] C. Canizares, T. Fernandes, E. Geraldi, L. Gerin-Lajoie, M. Gibbard, I. Hiskens, J. Kersulis, R. Kuiava, L. Lima, F. DeMarco, N. Martins, B. C. Pal, A. Piardi, R. Ramos, J. dos Santos, D. Silva, A. K. Singh, B. Tamimi, and D. Vowles, "Benchmark models for the analysis and control of small-signal oscillatory dynamics in power systems," *IEEE Trans. Power Syst.*, vol. 32, no. 1, pp. 715–722, Jan. 2017.

[2] A. T. Saric and A. M. Stankovic, "Rapid small-signal stability assessment and enhancement following changes in topology," *IEEE Trans. Power Syst.*, vol. 30, no. 3, pp. 1155–1163, May 2015.

[3] C. Li, Y. Cao, C. Duan, and K. Zhang, "A feasible delay margin sensitivity analysis method," *IEEE Trans. Power Syst.*, vol. 36, no. 3, pp. 2713–2716, May 2021.

[4] R. Krishan and A. Verma, "Assessment and enhancement of Hopf bifurcation stability margin in uncertain power systems," *Electr. Power Syst. Res.*, vol. 206, May 2022, Art. no. 107783.
[5] Y. Li, G. Geng, Q. Jiang, W. Li, and X. Shi, "A sequential approach for small signal stability enhancement with optimizing generation cost," *IEEE Trans. Power Syst.*, vol. 34, no. 6, pp. 4828–4836, Nov. 2019.
[6] J. Rommes, N. Martins, and F. D. Freitas, "Computing rightmost eigenvalues for small-signal stability assessment of large-scale power systems," *IEEE Trans. Power Syst.*, vol. 25, no. 2, pp. 929–938, May 2010.
[7] S. Gao, Z. Du, and Y. Li, "An improved contour-integral algorithm for calculating critical eigenvalues of power systems based on accurate number counting," *IEEE Trans. Power Syst.*, vol. 38, no. 1, pp. 549–558, Jan. 2023.
[8] C. Li, J. Wu, C. Duan, and Z. Du, "Development of an effective model for computing rightmost eigenvalues of power systems with inclusion of time delays," *IEEE Trans. Power Syst.*, vol. 34, no. 6, pp. 4216–4227, Nov. 2019.
[9] T. Y. Ji, X. Zheng, W. B. Lin, and L. L. Zhang, "Low frequency oscillation modal identification based on blind source separation considering uncertainty of modal parameters," *Electr. Power Syst. Res.*, vol. 214, Jan. 2023, Art. no. 108908.
[10] J. G. Philip, Y. Yang, and J. Jung, "Identification of power system oscillation modes using empirical wavelet transform and Yoshida–Bertecco algorithm," *IEEE Access*, vol. 10, pp. 48927–48935, 2022.
[11] S. A. N. Sarmadi and V. Venkatasubramanian, "Electromechanical mode estimation using recursive adaptive stochastic subspace identification," *IEEE Trans. Power Syst.*, vol. 29, no. 1, pp. 349–358, Jan. 2014.
[12] T. Wang, T. Bi, H. Wang, and J. Liu, "Decision tree based online stability assessment scheme for power systems with renewable generations," *CSEE J. Power Energy Syst.*, vol. 1, no. 2, pp. 53–61, Jun. 2015.
[13] F. Thams, A. Venzke, R. Eriksson, and S. Chatzivasileiadis, "Efficient database generation for data-driven security assessment of power systems," *IEEE Trans. Power Syst.*, vol. 35, no. 1, pp. 30–41, Jan. 2020.
[14] D. Shetty and N. Prabhu, "Performance analysis of data-driven techniques for detection and identification of low frequency oscillations in multimachine power system," *IEEE Access*, vol. 9, pp. 133416–133437, 2021.
[15] T. Jiang, Y. Mu, H. Jia, N. Lu, H. Yuan, J. Yan, and W. Li, "A novel dominant mode estimation method for analyzing inter-area oscillation in China Southern power grid," *IEEE Trans. Smart Grid*, vol. 7, no. 5, pp. 2549–2560, Sep. 2016.
[16] J. Zhang, C. Y. Chung, Z. Wang, and X. Zheng, "Instantaneous electromechanical dynamics monitoring in smart transmission grid," *IEEE Trans. Ind. Informat.*, vol. 12, no. 2, pp. 844–852, Apr. 2016.
[17] S. Liu, D. Mao, T. Xue, F. Tang, X. Li, L. Liu, R. Shi, S. Liao, and M. Zhang, "A data-driven approach for online inter-area oscillatory stability assessment of power systems based on random bits forest considering feature redundancy," *Energies*, vol. 14, no. 6, p. 1641, Mar. 2021.
[18] S. K. Azman, Y. J. Isbeih, M. S. E. Moursi, and K. Elbassioni, "A unified online deep learning prediction model for small signal and transient stability," *IEEE Trans. Power Syst.*, vol. 35, no. 6, pp. 4585–4598, Nov. 2020.
[19] S. P. Teeuwsen, I. Erlich, M. A. El-Sharkawi, and U. Bachmann, "Genetic algorithm and decision tree-based oscillatory stability assessment," *IEEE Trans. Power Syst.*, vol. 21, no. 2, pp. 746–753, May 2006.
[20] J. Liu, Z. Yang, J. Zhao, J. Yu, B. Tan, and W. Li, "Explicit data-driven small-signal stability constrained optimal power flow," *IEEE Trans. Power Syst.*, vol. 37, no. 5, pp. 3726–3737, Sep. 2022.
[21] R. Liu, G. Verbic, J. Ma, and D. J. Hill, "Fast stability scanning for future grid scenario analysis," *IEEE Trans. Power Syst.*, vol. 33, no. 1, pp. 514–524, Jan. 2018.
[22] S. Gurung, S. Naetiladdanon, and A. Sangswang, "A surrogate based computationally efficient method to coordinate damping controllers for enhancement of probabilistic small-signal stability," *IEEE Access*, vol. 9, pp. 32882–32896, 2021.
[23] S. Asvapoositkul, "Data-driven small-disturbance stability assessment and preventive control in mixed ACDC low inertia power systems," Ph.D. dissertation, Dept. Elect. Eng., Manchester Univ., Manchester, U.K., 2021.
[24] D. Yang, B. Wang, J. Ma, Z. Chen, G. Cai, Z. Sun, and L. Wang, "Ambient-data-driven modal-identification-based approach to estimate the inertia of an interconnected power system," *IEEE Access*, vol. 8, pp. 118799–118807, 2020.
[25] B. J. Frey and D. Dueck, "Clustering by passing messages between data points," *Science*, vol. 315, no. 5814, pp. 972–976, Feb. 2007.
[26] F. Milano. *Power System Analysis Toolbox (PSAT)*. Accessed: Jun. 6, 2022. [Online]. Available: http://faraday1.ucd.ie/index.html
[27] D. Z. Ray and E. M. Carlos. *A MATLAB Power System Simulation Package*. Accessed: Jan. 12, 2022. [Online]. Available: https://matpower.org/

XIN CUN received the B.S. degree in electrical engineering from Southwest Jiaotong University, China, in 2015, and the M.Sc. degree in electrical engineering from the School of Automation, Guangdong University of Technology, Guangzhou, China, in 2019. She is currently pursuing the Ph.D. degree in electrical engineering with Zhejiang University, Hangzhou, China.

In 2017, she was a Visiting Student with the Department of Engineering, University of Sannio, Benevento, Italy. Her research interests include small-signal stability, electricity market load forecasting, and machine learning.

XUNJUN CHEN (Member, IEEE) received the B.S. degree in electrical engineering and its automation and the M.S. degree in electrical engineering from Southwest Jiaotong University, Chengdu, China, in 2018 and 2021, respectively. He is currently pursuing the Ph.D. degree in power engineering with Zhejiang University, Hangzhou, China.

From 2017 to 2018, he was an Exchange Student sponsored by the China Scholarship Council with the Department of Electrical and Computer Engineering, Technical University of Munich, Munich, Germany. His research interests include the modeling of power electronics-based power systems and energy storage systems.

GUANGCHAO GENG (Senior Member, IEEE) received the B.S. and Ph.D. degrees in electrical engineering from Zhejiang University, Hangzhou, China, in 2009 and 2014, respectively.

From 2012 to 2013, he was a Visiting Student with the Department of Electrical and Computer Engineering, Iowa State University, Ames, IA, USA. From 2014 to 2017, he was a Postdoctoral Fellow with the College of Control Science and Engineering, Zhejiang University, and the Department of Electrical and Computer Engineering, University of Alberta, Edmonton, AB, Canada. From 2017 to 2019, he was a Research Assistant Professor with the College of Electrical Engineering, Zhejiang University, where he is currently an Associate Professor. His research interests include power nonintrusive sensing technology, data analytics in power systems, and power system stability and control.

QUANYUAN JIANG (Senior Member, IEEE) received the B.S., M.S., and Ph.D. degrees in electrical engineering from the Huazhong University of Science and Technology, Wuhan, China, in 1997, 2000, and 2003, respectively.

From 2006 to 2008, he was a Visiting Associate Professor with the School of Electrical and Computer Engineering, Cornell University, Ithaca, NY, USA. He is currently a Professor with the College of Electrical Engineering and an Academic Dean of the Graduate School, Zhejiang University, Hangzhou, China. His research interests include power system stability and control, applications of energy storage systems, and high-performance computing technique in power systems.